EVALUATION OF THE DYNAMIC APERTURE OF TARN II

A. Noda, M. Kanazawa\$, K. Noda, M. Yoshizawa and T. Watanabe
Institute for Nuclear Study, University of Tokyo
Midoricho 3-2-1
Tanashi-city, Tokyo 188, Japan

Abstract

Beam tracking has been performed for TARN II including the intrinsic sextupole components in the dipole magnets, which are smaller than 0.18 $1/m^3$ and the horizontal acceptance of 300 π mm·mrad is assured. The real structure of the field boundary requires almost twice as large as field gradient for vertically focusing quodrupoles compared with sharp edge model.

Introduction

An ion synchrotron - Cooler Ring, TARN II has been under construction since 1984 at Institute for Nuclear Study, University of Tokyo. Its layout is shown in Fig.1. It is close to the first beam circulation, which is scheduled at the end of this year. So as to prepare for such an operation, dynamic beam behaviour has been studied.

The mean radius of TARN II is 12.4 m and it can accept ion beams with magnetic rigidity up to 7 T·m, which corresponds to proton energy of 1.4 GeV. The injection energy is 20 MeV for proton and 2.7 MeV/u for Ne, which correspond to the magnetic rigidities of 0.65 T·m and 0.47 T·m, respectively. The peculiar feature to TARN II is rather wide range of excitation level (15 times) to be covered owing to the lower injection energy from the SF cyclotron with K-number 67 and the minimum injection field level becomes 0.12 T.

The vertical focusing in TARN II lattice is realized by 6 quadrupole magnets (Q_D) and edge focusing of 24 dipole magnets (B) whose edge angle is 7.5° at both entrance and exit. The effect of edge focusing is anticipated to be affected by the structure of the fringing field. So it is important to take the fringing field structure into account in the investigation of tune diagram.

In the present paper, the field properties of the dipole magnets by the field measurement are briefly summarized at first, then the beam tracking including the sextupole field in the dipole is described. Finally, the effect of the fringing field structure on the ring tune is presented.

Field Properties of TARN II Dipole

It is not the scope of this paper to describe in detail the field structure and the field measurement[1]. So only the necessary results to perform the beam dynamics study are to be presented.

Evaluation of the Sextupole Components

In Fig. 2, the typical structures of dipole field at various excitation levels obtained by flip coils are given. At field levels below 1.5 T, the sextupole components at the inner part of the magnet (measured with CENTER COIL) are small except for the lowest field level of 0.12 T, where the sextupole component at the inner part ($B''/B\rho$) becomes -0.06 ($1/m^3$) due to the presence of the remanent field. At the maximum field level of 1.9 T, the sextupole component at the inner part becomes as large as -0.12 ($1/m^3$)due to the effect of saturation of the iron core. The integrated sextupole component ($\int B'' ds/B\rho$) is also measured with LONG COIL simultaneously, which are -0.11 ($1/m^2$) and -0.18 ($1/m^2$) for the field level of 0.12 T and 1.9 T, respectively.

Because the quadrupole component is small for good reflection symmetry of our dipole magnet with H-type, the cross term between first order components in $\Delta L_0(x)$ and $\Delta B(x)$ is well assumed to be negligible, the following relation holds

$$\frac{\int B(x,s)ds}{B\rho} = \frac{L_0}{\rho}\left[1+\frac{\Delta L_0(x)}{L_0}+\frac{\Delta B(x)}{B_0}\right], \quad (1)$$

where $\Delta L_0(x)$ and $\Delta B(x)$ are the differences of the effective length(L_0) and the inner field strength(B) of the dipole magnet at the radial displacement of x from the ones at x=0, respectively. Utilizing Eq.(1), the sextupole component due to the curvature of the field boundary ($\Delta L_0''(x)/L_0$) can be derived from the sextupole components measured with LONG COIL ($\int B''(x,s)ds/\int B(0,s)ds$) and CENTER COIL ($B''(x)/B_0$). In table 1, thus obtained sextupole components are listed up for various excitation field levels.

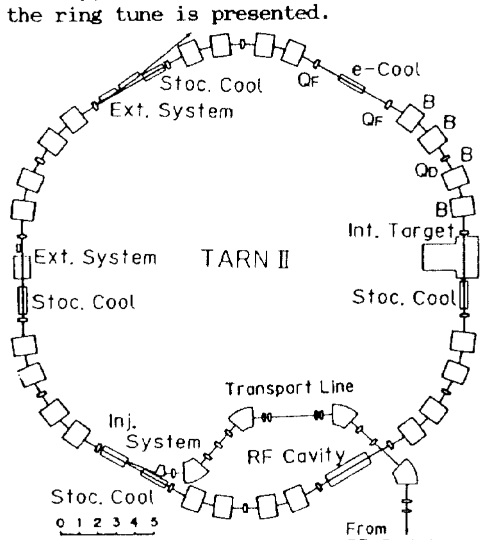

Fig. 1 Layout of TARN II.

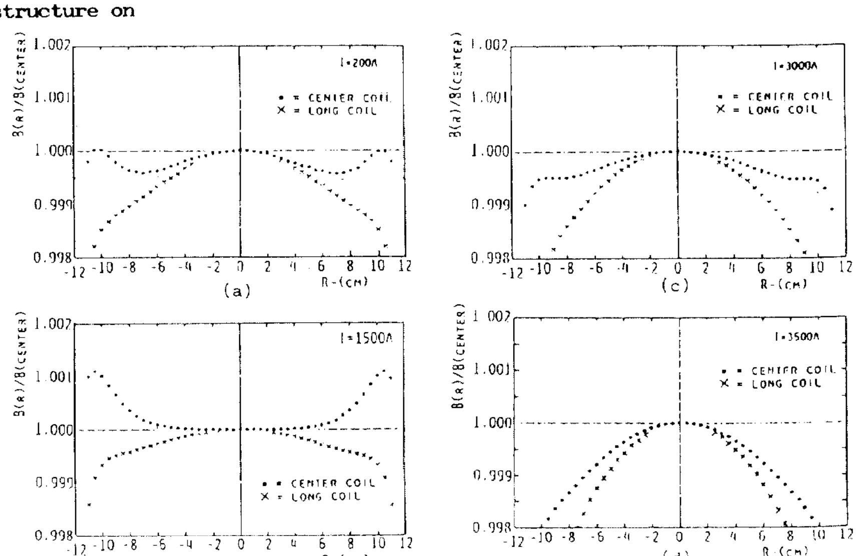

Fig. 2 Field Structure of TARN II Dipole Magnet.

\$ Present Address: Gesellschaft fuer Schwerionenforschung mbH, Darmstadt, Federal Republic of Germany

Table 1

Sextupole Components in Dipole Magnet

Excitation Current (A)	Magnetic Field (T)	Sextupole Components ($1/m^2$) Integrated ($\int B''ds/B\rho$)	Inner Part ($B''/B\rho$)	Edge ($\Delta L_0''/\rho$)
200	0.125	-0.11	-0.063	-0.024
1500	0.930	-0.04	0.011	-0.025
2500	1.55	-0.06	-0.026	-0.017
3000	1.74	-0.11	-0.074	-0.018
3500	1.90	-0.18	-0.116	-0.032

Fringing Field Structure

As shown in Fig. 3, the structure of the fringing field is measured by a Hall probe (Siemense FC 33) with temperature controle (Solid Line). Such a structure is also measured by a small flip coil (10 x 10 mm^2) which can be slided in the direction of magnet axis (Black Circle). Consistency between both systems are checked and is found to be very good.

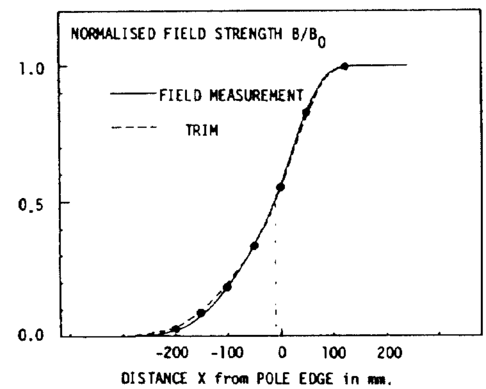

Fig. 3 Structure of the Fringing Field. (Solid Line; Measurement by a Hall Probe, Dashed Line; Calculation by TRIM, Black Circle; Measurement by a Flip Coil)

Beam Tracking

Beam tracking has been performed with use of MAD code[2] utilizing sextupole components given in Table 1. The sextupole component becomes maximum at highest field level of 1.9 T, but for this condition the beam size becomes rather small due to the shrinkage of the unnormalized emittance of the beam during acceleration. On the other hand, at the injection energy, the beam size is maximum and the sextupole is fairly large because of the remanent field. So the beam tracking was performed for the field levels of 0.12 T (injection) and 1.9 T (maximum energy).

In order to take the sextupole component in the dipole into account, the dipole magnet is virtually devided into 8 parts and thin sextupole with the strength of $B''L_0/4B\rho$ (SXC) is inserted as illustrated in Fig. 4. The effect of $\Delta L_0''/L_0$ is taken into account by attaching thin sextupoles of the strength of $\Delta L_0''/2\rho$ at the entrance and exit (SXE).

The starting coordinates are given at the center of the long straight section where the lattice has the

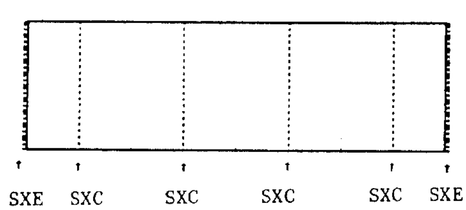

Fig. 4 Sextupole Components inherent in Dipole Magnet.

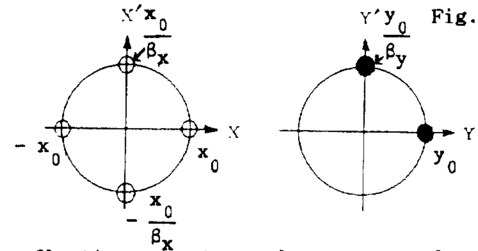

Fig. 5 Starting Coordinates for Tracking. Eight particles (4 x 2) are tracked.

reflection symmetry and α_x, α_y and η' are zero. In order to invesigate the effect of phase relation when these particles pass through the sextupole fields, starting coordinates in phase spaces are given as illustrated in Fig. 5. So as to evaluate the dynamically useful aperture of TARN II ring, the tracking was made for the various values of x_0 at the operating point of (1.755,1.202). In Fig. 6, an typical example of such tracking is shown. As is known from the figure, the beam motion is bounded even after many turns. However the maximum beam size becomes larger because of the kick by the sextupole field. Such kick is written as

$$\left.\frac{dx}{ds}\right|_2 - \left.\frac{dx}{ds}\right|_1 = -\frac{B''L}{2B\rho}(x^2 - y^2)$$
$$\left.\frac{dy}{ds}\right|_2 - \left.\frac{dy}{ds}\right|_1 = \frac{B''L}{B\rho}xy \qquad (2)$$

The kick in (x-x') phase space is almost cancelled after several turns because it does not include the betatron oscillation phase but only amplitudes, while the kick in (y-y') phase space includes the phases of betatron oscillations in x and y directions and add up to much larger amount (Fig. 6). Such a situation during 200 turns is shown in vertical transverse phase space in Fig. 7. In Fig. 8, the ratio of the emittance after these kicks (ε) to the initial one (ε_0) is plotted to x_0. Although the beam emittance increases in vertical direction, the beam emittance does not exceed the vertical acceptance of 30 π mm·mrad in the x_0 region of (-0.05 m, 0.05 m) corresponding to the acceptance of 300 π mm·mrad in horizontal direction.

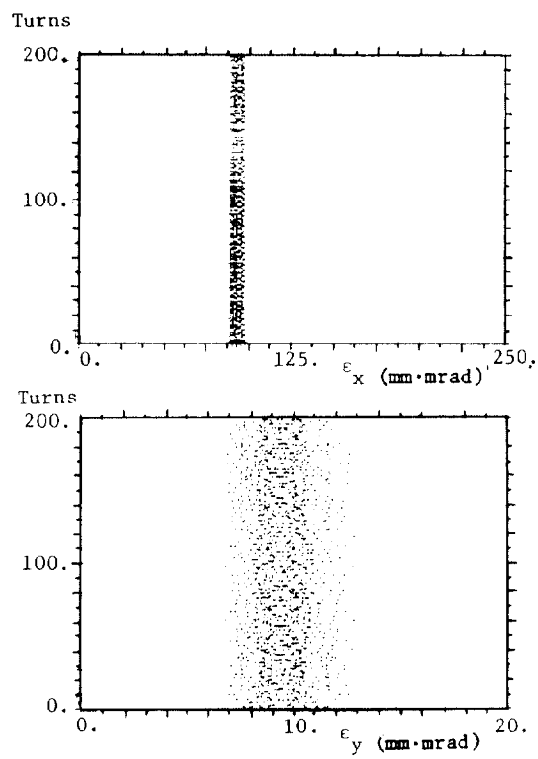

Fig. 6 Example of Beam Tracking. Initial values are 92 and 9 mm·mrad for ε_x and ε_y, respectively.

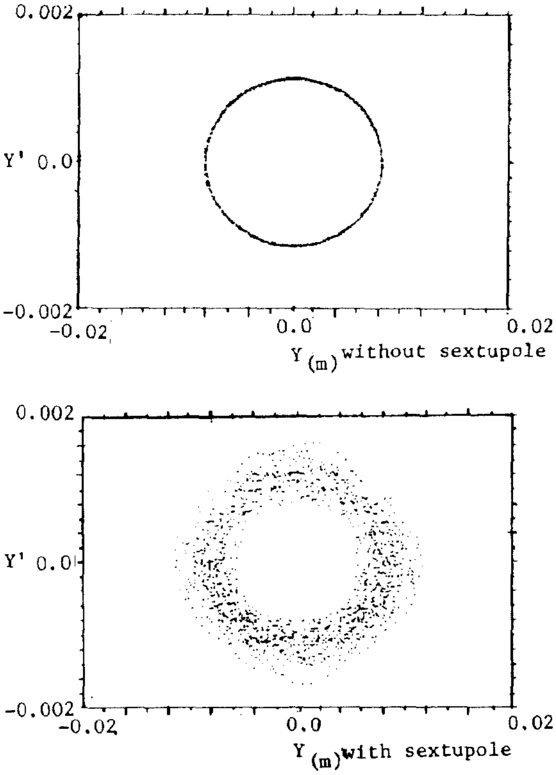

Fig. 7 Beam Behaviour during 200 turns in Y-Y' phase Space with(lower) and without(upper) intrinsic Sextupole Components in the Dipole Magnet.

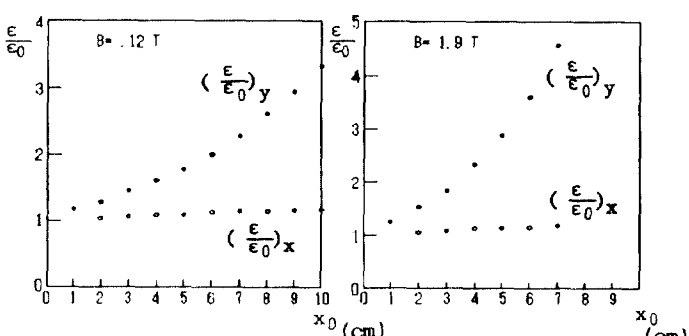

Fig. 8 Emittance Increase due to the Intrinsic Sextupoles in the Dipole Magnet for Various Starting Coordinates.

Effect of Fringing Field on Ring Tune

The effect of the fringing field is treated by K. L. Brown[3] in TRANSPORT code using the integral

$$K_1 = \int \frac{B_y(s)\,[\,B_0 - B_y(s)\,]}{gB_0^2}\, ds \,. \qquad (3)$$

This integral is numerically obtained from the measured data shown in Fig. 3, which resulted in 0.65 in good agreement with the value of 0.7 given for unclamped Rogowski magnet[4].

The correlation between focusing strength ($k=G/B\rho$) of the quadrupole magnets and ring tunes is investigated both for real structure of the field boundary and sharp edge approximation. As shown in Fig. 9, the field gradient needed to realize the same tune value for the case of real field boundary structure case is almost twice of that for the sharp edge case. It should be noted that if we utilize the sharp edge model for TARN II case in determination of the field gradients of quadrupole magnets, the tune error

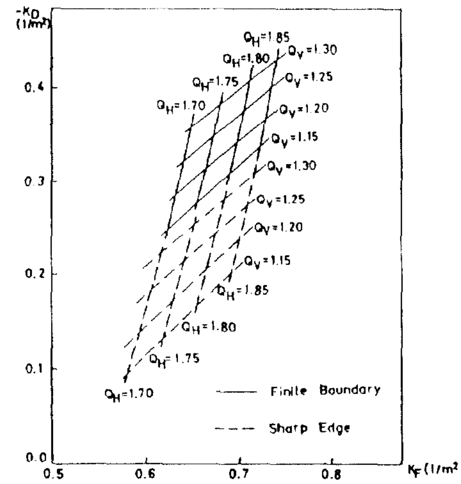

Fig. 9 Correlation between Focusing Strength of the Quadrupole Magnet Families and Ring Tunes calculated with real Field Boundary(Solid Line) and Sharp Edge Approximation(Dashed Line).

in vertical direction (ΔQ_y) amount to ~ -0.19, which might be very dangerous from the point of view of avoiding the resonance.

Such comparison is made also for TARN I, whose dipoles have normal entrance and exit. In TARN I case, the field gradients to realize the same operating point agree within a few percent between the real field boundary case and sharp edge approximation. So the sharp edge approximation is a good model only for the lattice with no edge focusing and careful study of fringing field structure is needed if the lattice assumes finite entrance and exit angle for the dipole magnets. This situation is particularly true for a small ring with small radius of curvature, ρ.

Aknowledgement

The authors would like to express their sincere thanks to all the members of TARN II construction group under the leadership of Profs. A. Mizobuchi and T. Katayama. They are also grateful to Prof. Y. Hirao for his continuous encouragement. Their thanks are also due to Mr. K. Omata who kindly took care of numerical calculation with MAD. One of the authors (A. N.) would like to present his sincere thanks to Prof. Dr. E. Jaeschke of Max-Planck Institut fuer Kern Physik at Heidelberg who had given him a good chance to collaborate on TSR where he had started such tracking studies. He is also grateful to Dr. M. Grieser of M.P.I. at Heidelberg for his collaboration on beam tracking for TSR, which had stimulated such a study of TARN II.

References

[1] A. Noda et al.,"Magnet System of Heavy Ion Synchrotron and Cooler Ring, TARN II", Proc. 11th Int. Conf. on Cyclotrons and their Applications, Tokyo (1987) pp. 284-287.

[2] F. C. Iselin, "The MAD Program", CERN-LEP-TH/85-15, (1985).

[3] K. L. Brown, "A First- and Second-Order Matrix Theory for the Design of Beam Transport Systems and Charged Particle Spectrometers", SLAC-75 (1967).

[4] K. L. Brown et al., "TRANSPORT A Computer Program for Designing Charged Particle Beam Transport Systems", CERN·80-04 (1980).